JOURNAL OF MATERIALS SCIENCE 31 (1996) 807–817

Diffusion bonding of an aluminium–lithium alloy (AA8090) using aluminium–copper alloy interlayers Part I *Microstructure*

A. UREÑA, J. M. GOMEZ DE SALAZAR, J. QUIÑONES, S. MERINO, J. J. MARTIN
Departamento Ciencia de los Materiales e Ingeniería Metalúrgica, Facultad de Ciencias Químicas, Universidad Complutense de Madrid, Spain

Diffusion bonds have been produced between sheets of an Al–Li–Cu–Mg–Zr alloy using aluminium–4% copper vapour deposited metallic interlayers. Microstructural changes occurred both in the parent alloy and in the bond interface after diffusion bonding cycles and post-bonding heat treatments were analysed. Different metallographic techniques (light microscopy, scanning and transmission electron microscopy) have been used. Diffusion bonding trials were carried out using the same alloy (AA8090), both in non-superplastic (T6) and superplastic conditions. Differences in their behaviours in relation to diffusion bonding were observed.

1. Introduction

The combination of superplastic forming (SPF) with diffusion bonding (DB), and its application to titanium alloys has meant the development of a widespread fabrication procedure of complex structures for aerospace application [1, 2]. However, to date, diffusion bonding of aluminium and its alloys shows important difficulties which avoid the application of SPF–DB in the fabrication of structural aluminium based alloy components for the aircraft industry.

The main problem for solid state bonding of aluminium is the presence of a protective oxide film (Al_2O_3) on the metal surface. This oxide has great stability and tenacity, beside very limited solubility into the metal matrix, even at high temperatures [3, 4]. Alumina film prevents the formation of metallic contacts during diffusion bonding and acts as a diffusion barrier. It avoids the achievement of high quality joints.

Aluminium–lithium alloys show similar bonding problems to other aluminium alloys. Some authors [5, 6] have reported that the high oxidizing tendency of these alloys makes diffusion bonding difficult. However, lithium, because of its high activity, forms less stable oxide films [7] and under the appropriate bonding conditions can accelerate oxide film disruption, making solid state bonding easy [8, 9].

Several methods have been proposed for diffusion bonding of aluminium–lithium alloys:

1. direct diffusion bonding without interlayers by application of high bonding pressures to break the oxide film, but promoting high overlap deformation [10];
2. liquid phase diffusion bonding using Cu and Zn interlayers [11]; or
3. solid state diffusion bonding with a copper interlayer, using long bonding times [12].

The present authors propose a solid state bonding method which uses an aluminium alloy as the interlayer and makes possible the achievement of high structural quality joints with very short bonding times. This method is developed for an AA8090–T6 without superplastic properties, and afterwards is applied to the same alloy but with superplastic behaviour. Detailed examination of the microstructural changes occurring in both parent sheets (grain growth, precipitation phenomena, grain boundary melting phenomena, lithium depleted surface formation, etc.) is carried out. Light microscopy (LM), scanning electron microscopy (SEM), transmission electron microscopy (TEM) and energy dispersive X-ray analysis (EDX) are used for these purposes. The results of these studies are reported in Part I of this paper. Shear and peel strength data and fracture behaviour will be described in Part II.

2. Experimental procedure

The parent material used for this investigation was an 8090 aluminium alloy with a composition (wt %) of Al–2.4 Li–1.12 Cu–0.82 Mg–0.06 Zr–0.04 Fe–0.02 Si–0.024 Ti. Material was supplied in the form of 1.5–3.0 mm thick sheets. Two different microstructural conditions were studied: a non-superplastic (8090–T6) and a thermochemically treated (8090–SP) one with superplastic properties.

Before the bonding trials, parent alloys were subjected to different heat treatments, which simulated the thermal bonding cycles (at 530 °C for 5–40 min, followed by slow cooling) and post-bonding heat treatments. The objective of these trials was to study

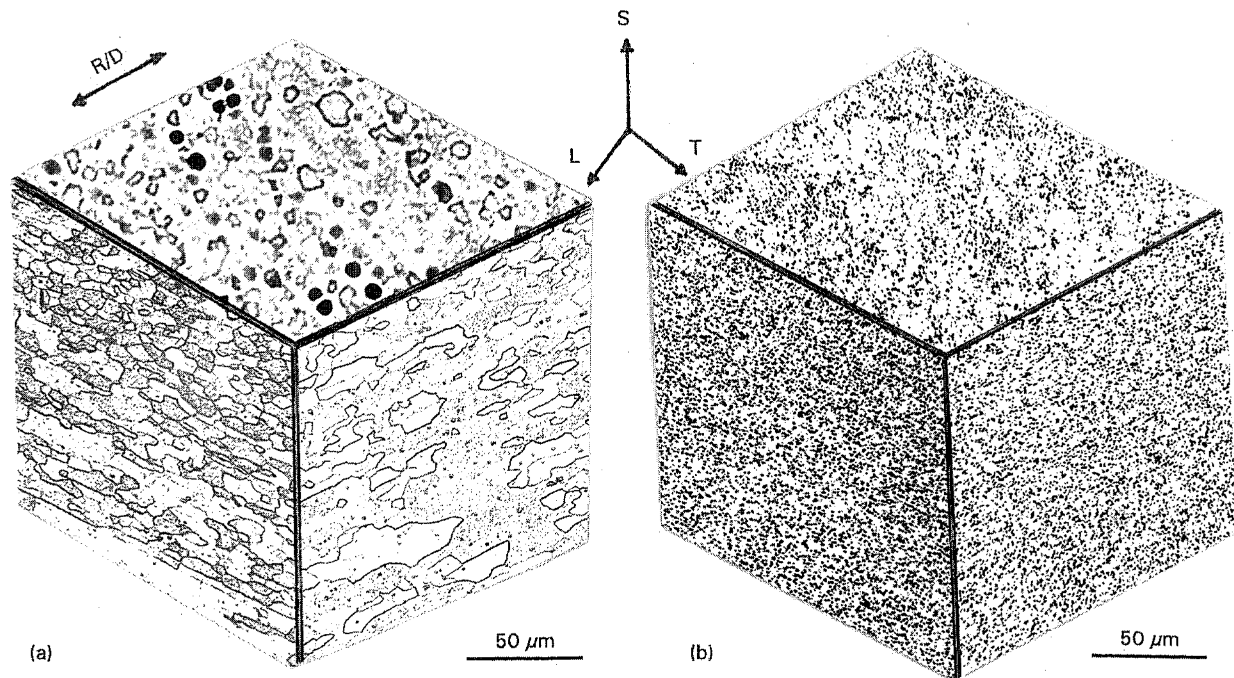

Figure 1 Three-dimensional micrographs of Al–Li alloys (etched in Keller reagent): (a) 8090–T6, and (b) 8090–SP (R/D, rolling direction).

the microstructural changes occurring in the parent sheets due to the thermal cycles applied during bonding.

Sheet surfaces to be bonded were mechanically ground on 600 grade SiC emery paper to obtain a roughness, (RA) of 0.4 μm. Specimens were ultrasonically washed in acetone to produce appropriate degreasing. A chemical cleaning treatment with a commercial deoxidant, generally used in aluminium alloys to produce uniform surfaces free of oxide and unsoluble salts, was also applied to some specimens prior to interlayer deposition. Prepared surfaces were coated with thin films (≈ 1 μm) of an aluminium–copper alloy (AA2024) by vapour deposition, in a high vacuum unit (10^{-3} Pa).

Diffusion bonding trials were carried out in a vacuum furnace by joining two sheets of identical thickness during short bonding times (5–30 min). A bonding temperature of 530 °C and low cooling rates were applied ($0.1\,°C\,s^{-1}$). Occasionally, temperatures higher than 530 °C were also used. The bonding pressure was varied in the range 1.5–8.0 MPa, and fixed at 5.5 MPa to give a final overall thickness deformation of 10–15% for diffusion bonding of the non-superplastic material. However, for the same bonding conditions, the final deformation introduced in the superplastic 8090 diffusion bonds was always higher than 30%. Bonding trials were carried out in a protective atmosphere with vacuum levels down to 10^{-2} Pa ($P_{O_2} \approx 2 \times 10^{-3}$ Pa).

Bonds were examined both in the as-bonded condition and after different post-bonding heat treatments. These treatments consisted of a solution heat treatment (SHT) at 530 ± 5 °C for 2 h with cold water quenching, followed by natural (T4) or artificial ageing (T6) at 190 ± 1 °C for 8 h. Solution heat treatments were carried out both in an air and argon furnace. Artificial ageing was applied in the thermostatic glycerine baths.

Transverse sections were prepared from diffusion bonds and the treated parent materials by conventional metallographic techniques. Studies of grain growth by quantitative metallographic techniques and measuring of the lithium depleted zones formed by oxidation during bonding and heat treatment were carried out.

Besides conventional studies with LM and SEM, both joints and parent sheets were observed by TEM. Specimens for TEM were prepared by mechanical grinding down to thicknesses of 100–150 μm, followed by electrolyte solution at -10 °C with a potential difference of 15–20 V, to obtain films of ≤ 30 μm [13]. Afterwards, the films were finished by electropolishing using twin jet polishing equipment. Samples were subsequently examined in a Jeol 200 kV microscope equipped with energy dispersive X-ray spectroscopy (EDX) facilities.

3. Results

3.1. Microstructure of parent material

Three-dimensional light micrographs of the as-received microstructures in the T6 and superplastic 8090 alloys are shown in Fig. 1a, b, respectively. In general, they reveal unrecrystallized grain structures typical of thermomechanical processing, with pancake shaped grains elongated in the rolling direction. However, 8090–SP is much finer grained and presents a higher density of equilibrium precipitates of 1–2 μm diameter, whereas 8090–T6 shows some degree of recrystallization, especially in zones close to the sheet surfaces.

Further microstructural examinations using TEM revealed the existence, in the 8090–SP alloy, of a fine

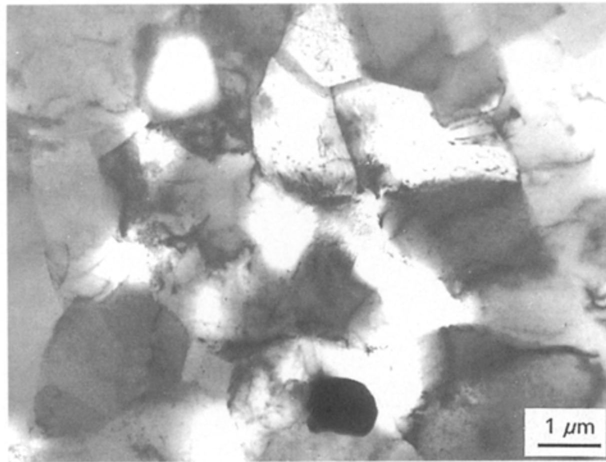

Figure 2 TEM image of 8090–SP alloy microstructure showing ultrafine grains (1–2 μm).

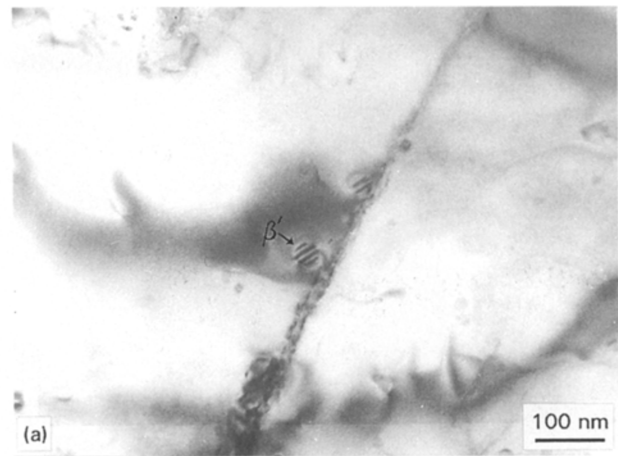

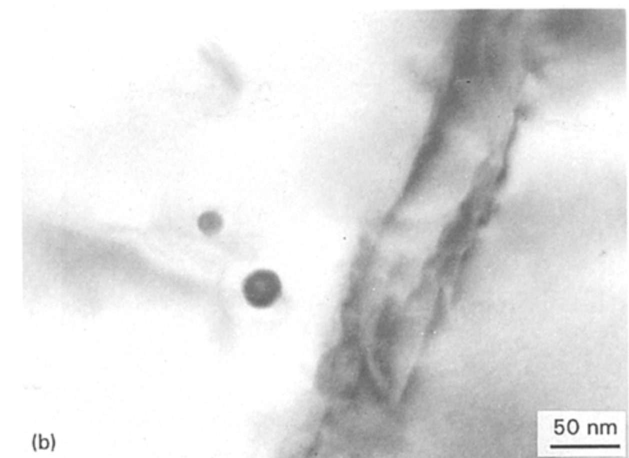

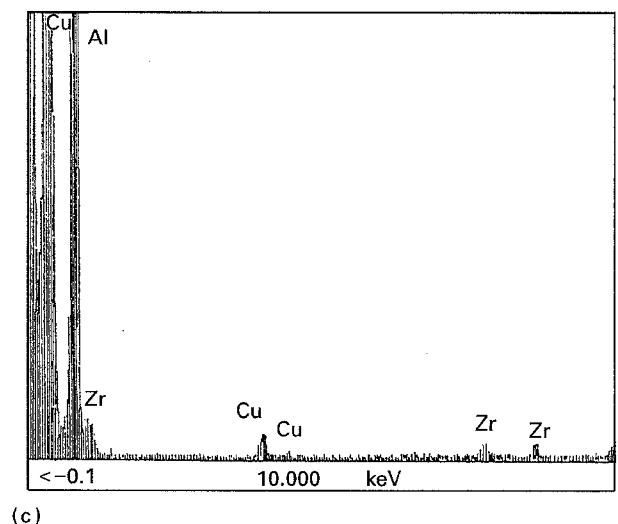

Figure 3 β′(Al_3Zr) dispersoids in 8090 SP alloy: (a) in grain boundaries, (b) inside the grains, and (c) EDX microanalysis of Al_3Zr precipitates.

equiaxed subgrain structure, approximately 1 μm in diameter, within the unrecrystallized grains (Fig. 2). Metastable cubic Al_3Zr (β′ phase) precipitates, identified by EDX (Fig. 3a), were observed in grain boundaries (Fig. 3b) and within the grains of the alloy (Fig. 3c). They are usually spherical in morphology and can effectively pin the grain and subgrain boundaries. Rows of β′ particles have also been observed in grain boundaries of the non-superplastic sheet (8090–T6) (Fig. 4).

Both studied materials also present other minority precipitates which have been found within the grains (Fig. 5a). EDX microanalysis of these particles showed the presence of significant amounts of Fe and Si, respectively (Fig. 5b, c). Both elements are present in the alloy as impurities, and they precipitate during ingot solidification as insoluble constituent phases (Al_7Cu_2Fe, Al_3Fe, Si, etc.).

3.2. Microstructural changes occurring in the parent sheets during solid state bonding

3.2.1. Phase precipitation

Microstructural studies carried out both in the as-bonded sheets and in the heat treated ones with simulated bonding cycles, showed the precipitation of equilibrium phases for the AA8090. Fig. 6a, b show isothermal sections through the ternary Al–Cu–Li phase diagram, adapted from various sources [14], at 350 °C and close to the bonding temperature (500 °C). Heterogeneous precipitation of a high volume fraction of the equilibrium phases LiAl (δ) and $CuLi_3Al_6$ (T_2) is favoured during slow cooling ($\simeq 0.1\,°C\,s^{-1}$) from the bonding temperature. It also produces a coarsening of these precipitates, especially those located in the grain and subgrain boundaries (Fig. 7a, b). This phenomenon occurred also in the as-bonded 8090–SP alloy. However, particles keep their original band orientation developed by thermomechanical processing, because of high stability of the grain structure.

In both cases, solubilization of those equilibrium particles can be generated by application of a post-bonding solution heat treatment (530 °C for 2 h) followed by water quenching. Maximum strength in both alloys can be obtained after the application of artificial ageing (see Part II). Artificial ageing was carried out at 190 °C following the recommendations of several authors [15]. However, microstructural studies of artificially aged diffusion bonds of 8090–SP showed the precipitation of δ and T_2 in grain bound-

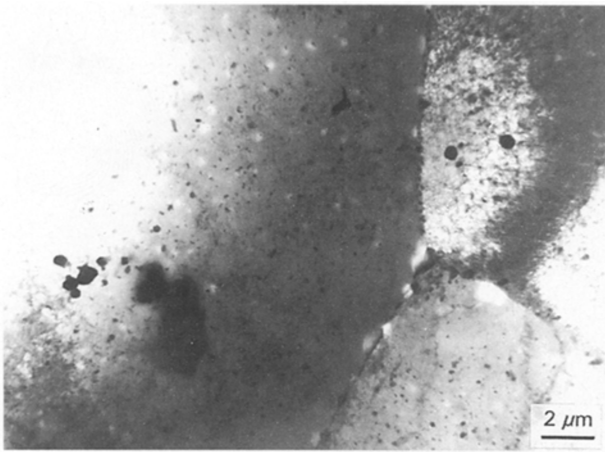

Figure 4 Rows of Al_3Zr particles in grain boundaries of 8090–T6 alloy.

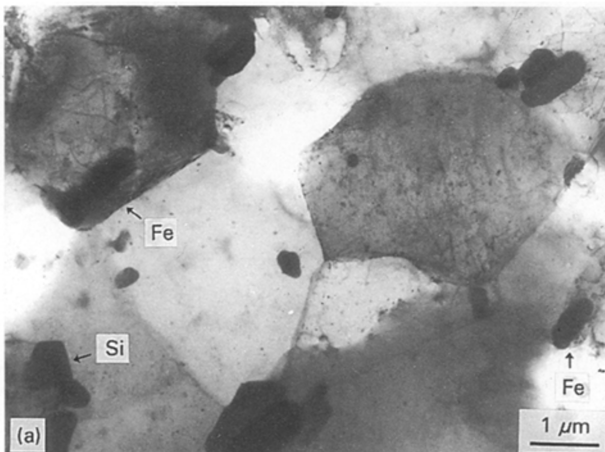

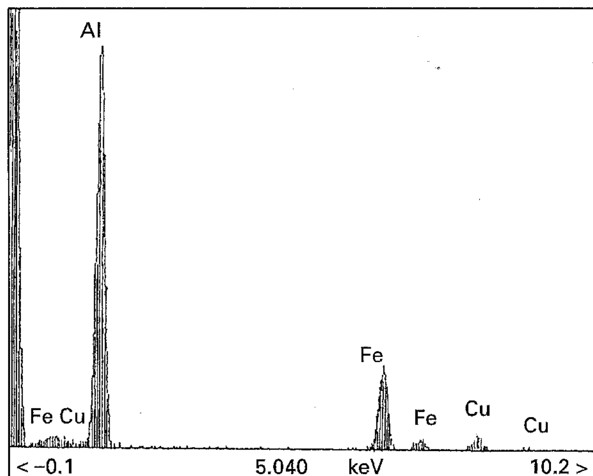

(b)

Figure 5 (a) Fe and Si-rich phases in 8090–T6 alloy, (b) EDX of Fe–Cu–Al precipitates, and (c) EDX of Si aggregates.

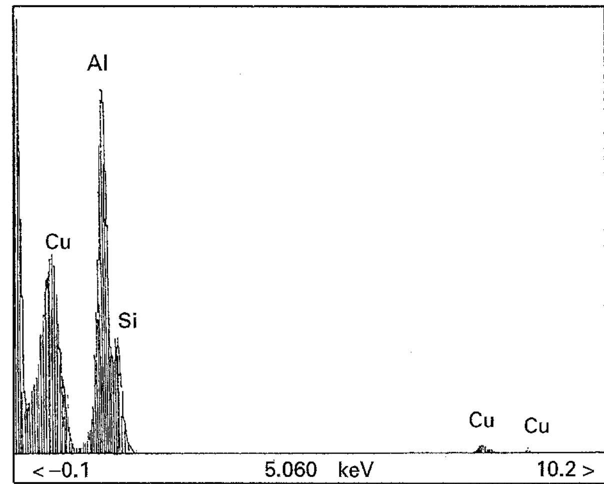

(c)

Figure 5 continued

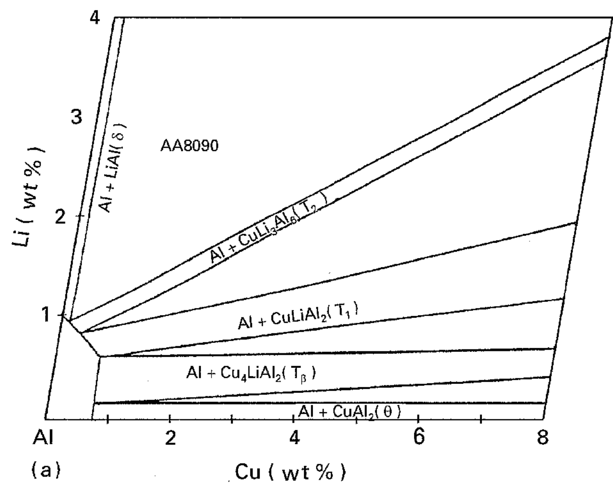

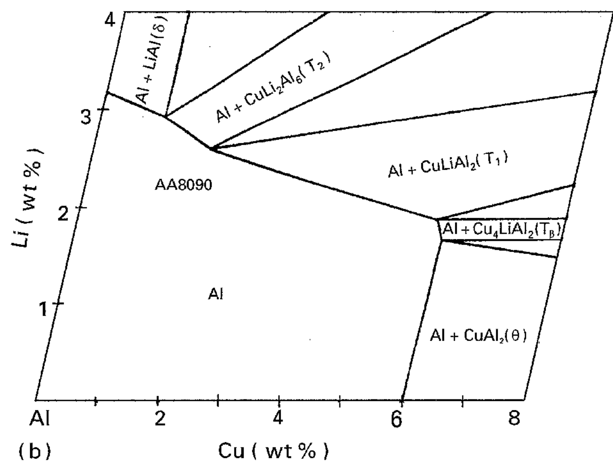

Figure 6 Isothermal sections of the Al-rich corner of the Al–Cu–Li phase diagram at (a) 325, and (b) 530 °C.

aries (Fig. 8) due to an overageing process. Therefore, the ageing temperature for this material was decreased to 170 °C.

3.2.2. Surface depletion of lithium

Several investigators [16, 17] have studied the surface oxidation of Li from Al–Li alloys during heat treatment. Formation of Li depleted surfaces by oxidation depends on the heat treatment conditions and the atmosphere in which it is carried out. Microstructural studies and microhardness measurements carried out for the present authors show that bonding cycles followed by post-bonding heat treatments are responsible for Li depletion from the surface.

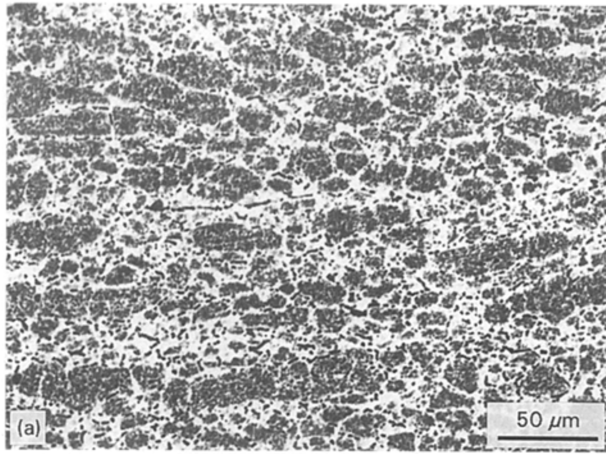

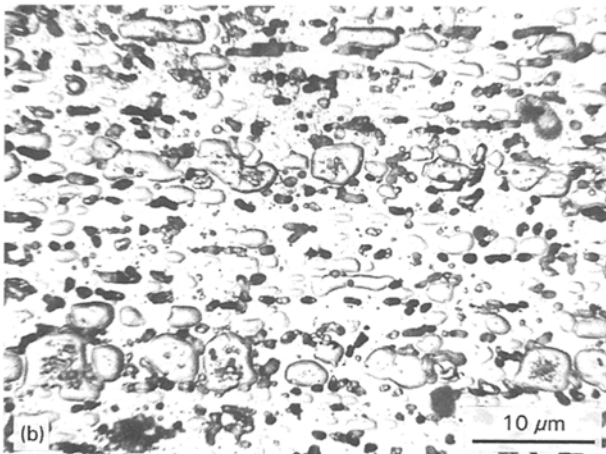

Figure 7 Heterogeneous precipitation of equilibrium phases into slow cooled aluminium–lithium alloys from the bonding temperature (530 °C): (a) 8090–T6 alloy, and (b) 8090–SP alloy.

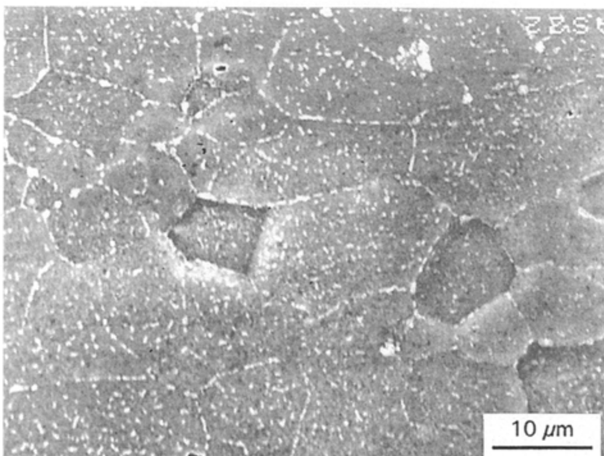

Figure 8 Overaged microstructure of 8090–SP alloy with coarsening of precipitates.

Since lithium is a very light element, its chemical analysis is not as easy as for other heavier elements. To overcome this problem an indirect method [16], measurement of microhardness from the sheet surface inwards, in bonded specimens which have been aged after the same solution heat treatment, was applied to determine the extent of Li loss.

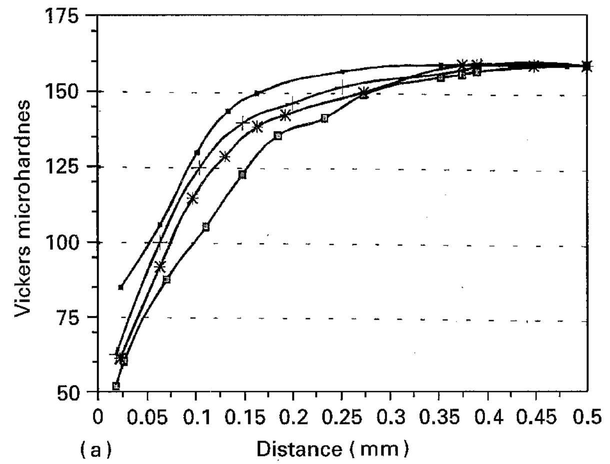

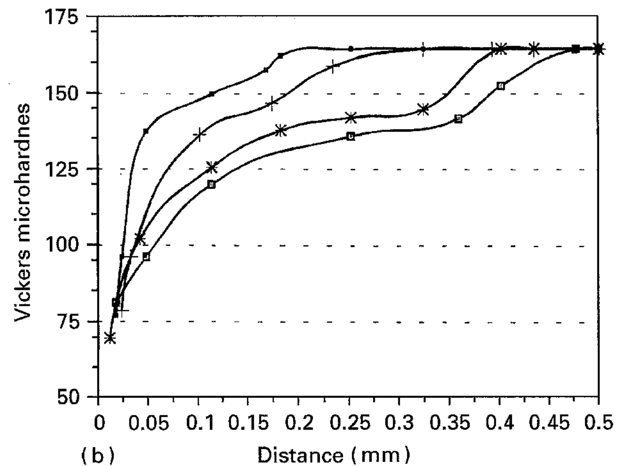

Figure 9 Vickers microhardness profiles showing lithium depletion from the alloy surfaces for different bonding times: (a) 8090–T6, and (b) 8090–SP: (■) 5, (+) 10, (*) 20, and (▤) 40 min, respectively.

The lithium concentration profiles for the two aluminium–lithium alloys were generated (Fig. 9a, b) as described before by plotting Vickers microhardness versus depth from the surface, for different bonding-times. The depth of Li depletion was considered to be the distance from the surface at which the hardness becomes constant. It was found that increasing the bonding time produces a larger depth of Li depletion and accentuates the hardness reduction. This phenomenon is more extended in the 8090–SP alloy.

Fig. 10 shows the depth of Li depletion versus bonding time for both Al–Li alloys. However, it is necessary to consider the contribution to these values of the Li depletion produced during solution heat treatment. Besides, the initial depth of Li depletion measured in the as-received sheets (100 and 60 μm for 8090–T6 and 8090–SP alloys, respectively) may be considered.

This phenomenon has also been observed by microstuctural studies of as-bonded sheets, because the formation of a precipitate depleted band suggest that the lithium concentration was below 1.0 wt % [16]. This band widens with increasing bonding time (Fig. 11a, b). It has also been observed that the combined effects of solute depletion and high temperatures

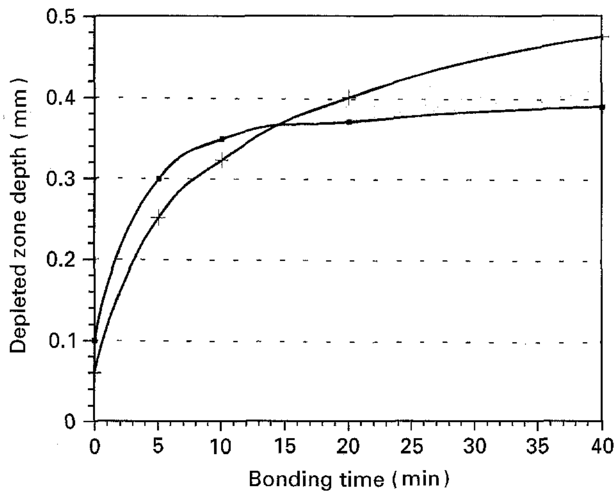

Figure 10 Depth of Li depletion versus bonding time or both studied Al-Li alloys: (■) 8090–T6, (+) 8090–SP.

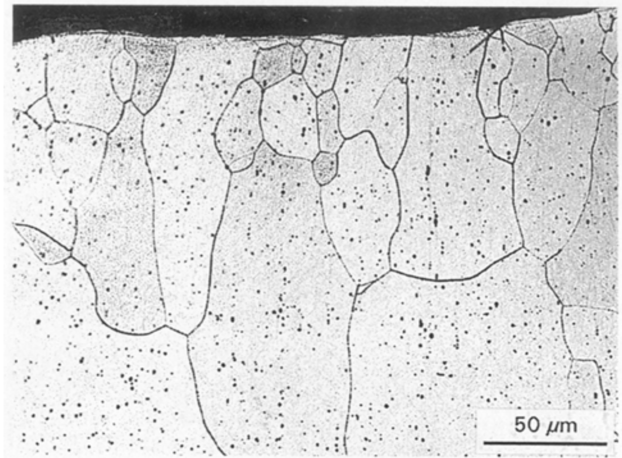

Figure 12 Recrystallization and grain growth at the alloy surface caused by the combined effects of solute depletion and high temperature.

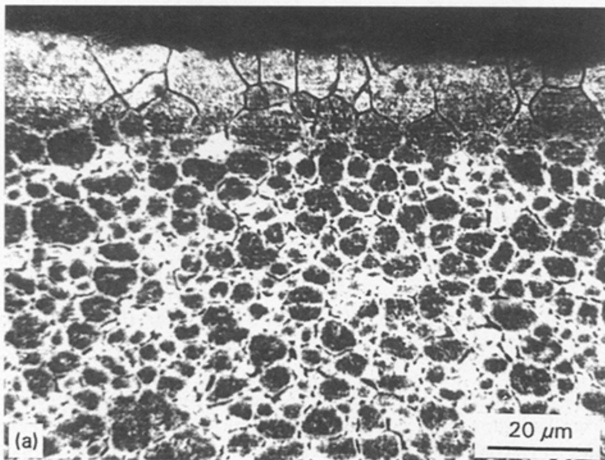

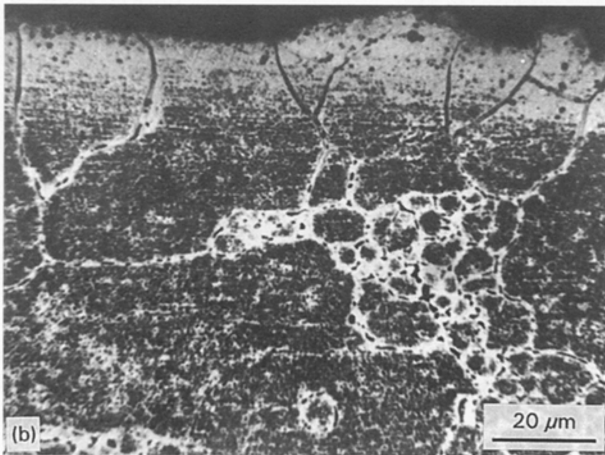

Figure 11 Surface microstructure of bonding cycled material at 530 °C for (a) 10 min, and (b) 40 min followed by furnace cooling.

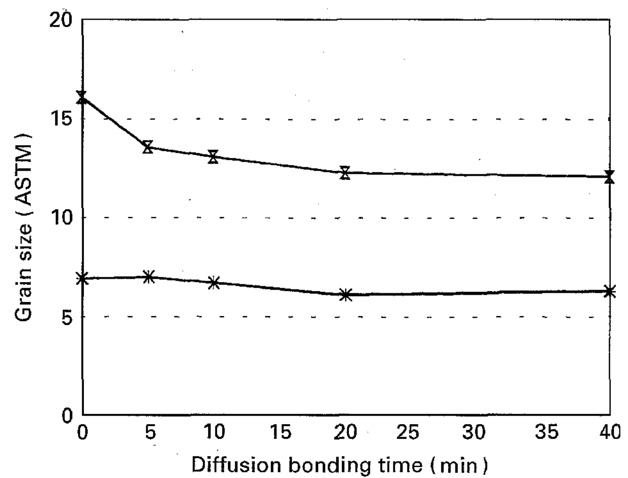

Figure 13 Grain size versus bonding time for (∗) 8090–T6 and (⧖) 8090–SP alloys.

caused recrystallization and grain growth at the surface (Fig. 12).

3.2.3. Grain size stability

The influence of the bonding cycle on the grain size of the 8090 alloy has been studied to deduce if the bonding procedure generates recrystallization and coarsening of the grain size. To generate superplastic flow it is necessary to keep the grain size within the range 3–10 μm [18].

Fig. 13 represents the grain sizes measured by morphometric techniques using a quantitative analyser versus bonding time. For the 8090–T6 alloy, the grain size was kept almost constant in the nominal diameter range of 50–60 μm (6.7–7.2 morphometric ASTM). However, the grain size for the 8090–SP sheet increases from 2.5 μm up to values slightly higher than 10 μm, when the bonding time is longer than 30 min. In spite of this the effect of the β′ precipitates is enough to keep the grain size of the alloy in the range of superplastic behaviour.

When the bonding temperature was increased to values higher than 550 °C, incipient melting in grain boundaries was observed. In these cases, the grains experienced great growth because of the loss of the pinning effect of Al_3Zr precipitates.

3.3. Microstructure of solid state bonded interfaces

3.3.1. Diffusion joints in 8090–T6 alloy

The characteristic microstructure of a diffusion bonded 8090–T6 sheet, in the as-bonded condition, is

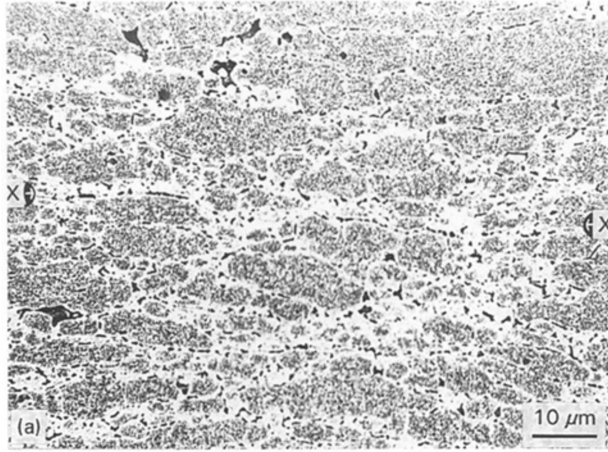

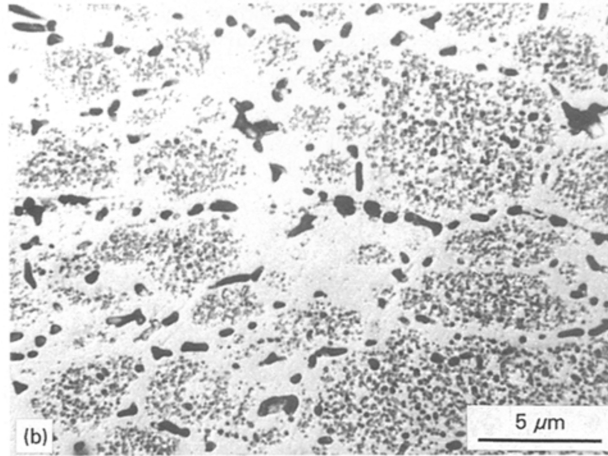

Figure 14 (a) Optical micrography of an as-bonded 8090–T6 joint using a copper–aluminium interlayer (interface at X–X), and (b) detail of equilibrium precipitates coarsed at grain boundaries and bonding interface.

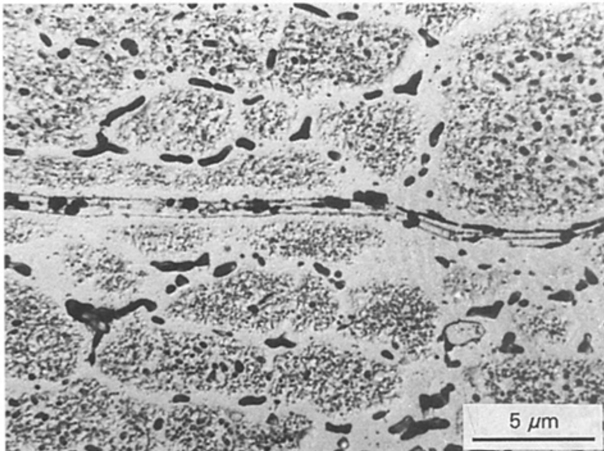

Figure 15 Al–Cu interlayers still visible in a 8090–T6 diffusion joint bonded at 530 °C for 5 min and 4 MPa.

shown in Fig. 14a, b. The alloy element precipitation described in Section 3.2. occurred preferentially in the bond interface, and showed a similar morphology to that of the adjacent grain boundaries. The aluminium–copper interlayer generally disappeared. Only in specimens bonded with very short bonding times ($\simeq$ 5 min) or low pressures ($<$ 4 MPa) which experienced deformation of less than 10%, are both intermediate films still visible (Fig. 15). On the other hand,

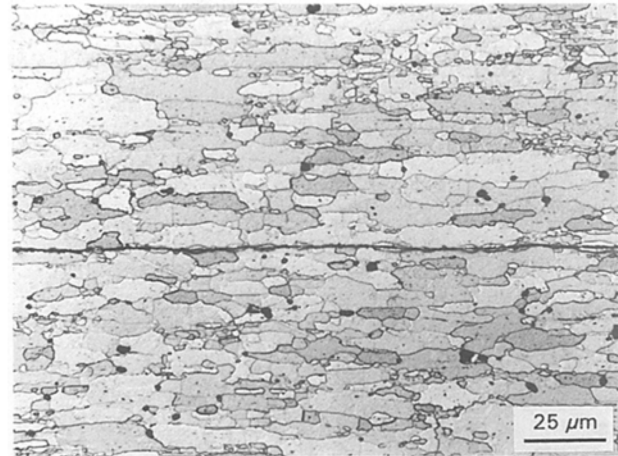

Figure 16 Post-bonding heat treated diffusion joint bonded with low deformation ($\leqslant$ 10%). Formation of continuous interface oxide layer is observed.

the formation of an interfacial continuous oxide layer was observed when bonding trials were made in an oxidizing atmosphere ($P_{O_2} > 2 \times 10^{-3}$ Pa).

Application of the post-bonding heat treatment previously described (SHT + Q + ageing) to the joints, produced redissolution of the alloying precipitates and recovered the parent alloy microstructure. However, complete dissolution of the interface precipitated was not always possible.

In diffusion joints bonded with low deformation ($\leqslant$ 10%), the insolubilized particles formed an almost continuous film (Fig. 16), conferring a very low quality to the joints. Increasing the bonding deformation, the film tends to disrupt forming isolated particles with spheroidal morphologies (Fig. 17a). These particles have been identified by EDX (Fig. 17b) as complex oxides of aluminium, probably containing lithium. Table I shows the possible chemical reactions between lithium and the aluminium oxide film [16].

Although to produce complete elimination of the oxide remains, it is necessary to work with high deformation ($>$ 25%), it has been observed that using bonding surfaces which were previously chemical treated, the final proportions of oxide particles for low deformation can be reduced. It is possible, even in those cases where very low diffusion bonding pressures and times of 10 min (bonding deformation ($\leqslant$ 10%) were applied, that initial interlayers are still visible (Fig. 18).

For chemically treated specimens, bonded with deformations close to 15%, grain growth across the bond interface was observed. However, the grain growth always kept a planar configuration, similar to the conventional large-angle grain boundaries present in the sheet (Fig. 19). Even at high magnification, the bond interface showed no evidence of porosity or of a continuous interfacial oxide (Fig. 20a, b). These processes are accompanied by spheroidization of the oxide remains.

TEM studies have proved that homogenization of the interlayer across the bond interface was not always complete. It was especially observed in those cases where bond deformation was lower than 15% and

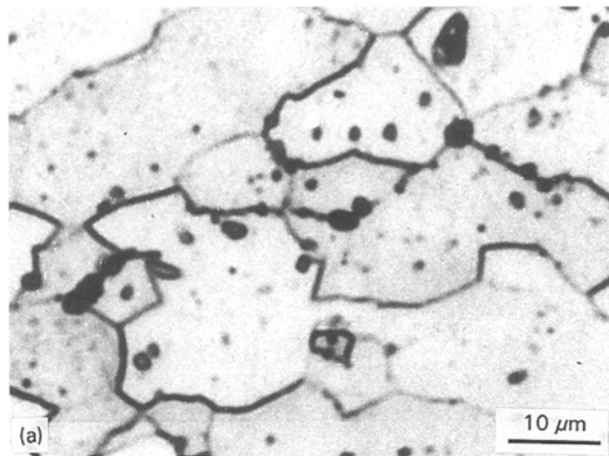

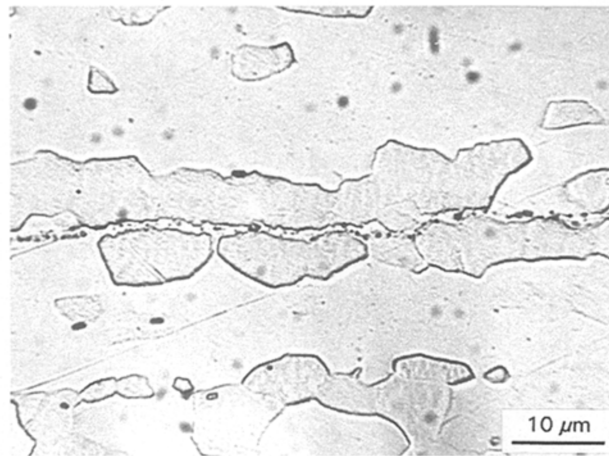

Figure 18 Micrograph of a low deformed diffusion bond with a previous surface chemical cleaning treatment (CCT).

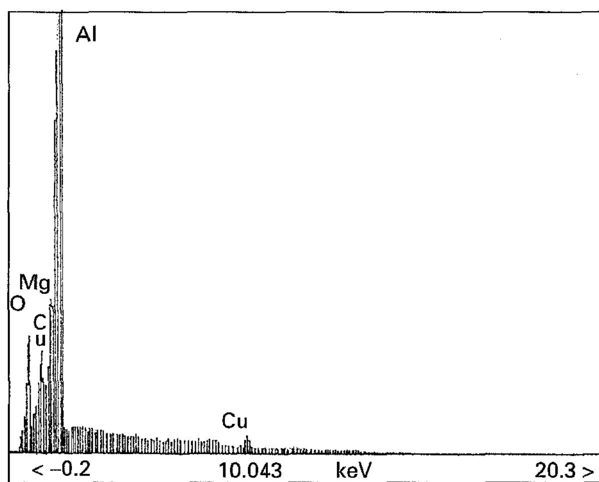

Figure 17 (a) Spheroidal oxides remains in the bond interface of a high thickness reduction joint (> 25%), and (b) EDX of oxide particles.

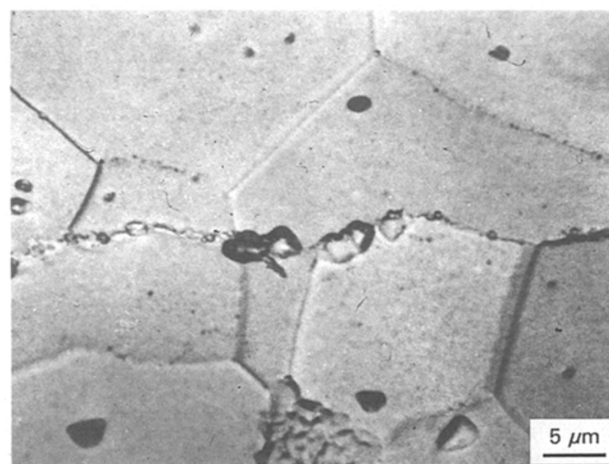

Figure 19 Bond interface in a CCT joint showing low oxide proportion and planar configuration.

TABLE I Possible reactions at bond interface with formation of Al–Li oxides (Free energy, $\Delta G°$ kJ mol^{-1}, at 530 °C)

Reactions	$\Delta G°$ at 530 °C (kJ mol^{-1})
$Li + 1/3Al_2O_3 \rightleftarrows LiO_2 + 2/3Al$	− 19
$Li + 8/3Al_2O_3 \rightleftarrows LiAl_5O_2 + 1/3Al$	− 36
$Li + 2/3Al_2O_3 \rightleftarrows LiAlO_2 + 1/3Al$	− 68

bonding times were 10 min. However, even in these cases, the interlayer exhibits an important thickness reduction and high continuity with the parent alloy can be obtained. Fig. 21 shows a transmission electron micrograph of one of these bond interfaces with a large particle of T2 phase (Al_6CuLi_3) present in it.

3.3.2. Diffusion joints in 8090–SP materials

Microstructural studies of diffusion bonded 8090–SP sheets show that the formation of aluminium–lithium oxides from the protective alumina films and their subsequent solubilization at the bonding conditions is more favoured than in the T6 materials. Fig. 22 is an optical micrograph of a post-bonded treated joint where the proportion of isolated oxide particles in the bond interface is lower than that observed in the non-superplastic 8090 alloy for the same bonding conditions. With these characteristics, the planar bond interface is difficult to distinguish from the surrounding grain boundaries.

However, the higher plasticity of this material at the bonding temperature makes it difficult to control the reduction of thickness. Values higher than 25% are obtained for the same bonding parameters used for 8090–T6 sheet (5.5 MPa, 10–30 min and 530 °C) for which the deformation was reduced by 10–15%. Besides, although the grain boundary migration did not occur in a complete way across the bond line, numerous recrystallization zones were observed. The proportion of these zones is higher than in the T6 material (Fig. 23).

SEM micrographs of bond interfaces for 8090–SP alloy show important differences in relation to the 8090–T6 material. First, although complete elimination of the Al–Cu interlayer is not always reached, it is more favoured than in non-superplastic sheet (Fig. 24a). Even in those zones where an interlayer is still distinguished, the interlayer shows an important thickness reduction with the small grain size produced

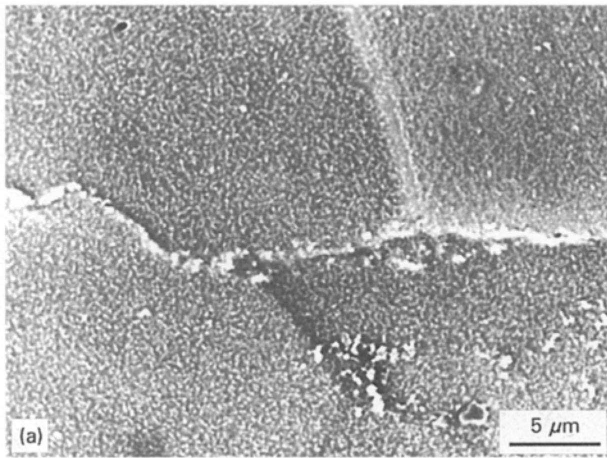

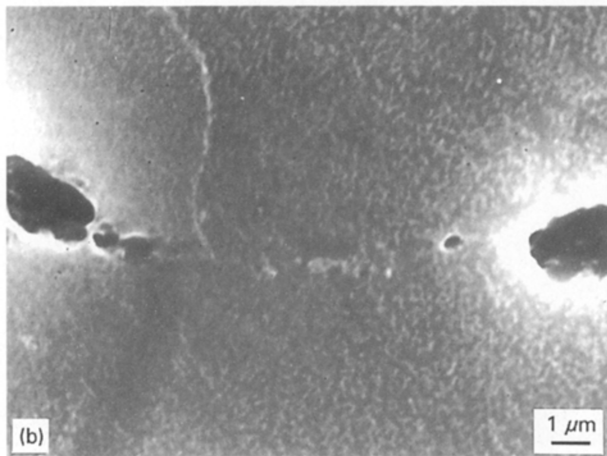

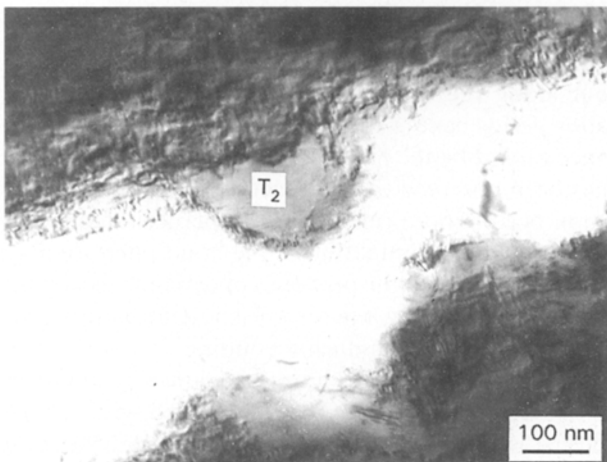

Figure 21 TEM image of the bond interface between Al–Li alloy and Al–Cu interlayer. T_2 particle at bond interface is marked.

by the recrystallization processes (Fig. 24b). TEM studies of those zones show this recrystallization phenomenon in the interlayer (Fig. 25a) and the formation of a new subgranular structure can be observed when it disappears (Fig. 25b).

The second fact observed is that there are numerous zones where the bond interface appears as a convectional gain boundary (X–X in Fig. 26). In those zones,

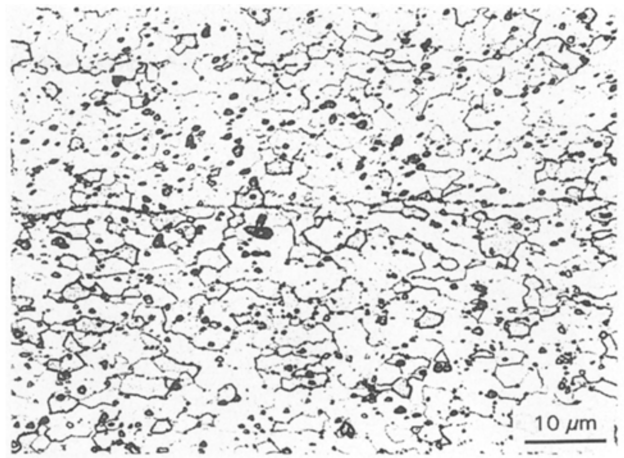

Figure 22 Typical microstructure of a 8090–SP diffusion bond.

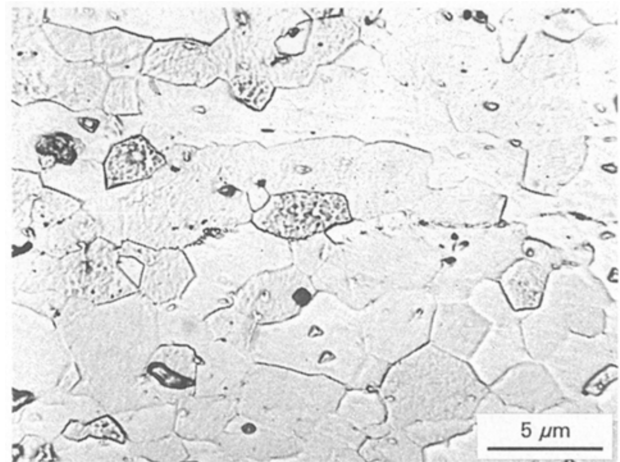

Figure 23 Detail of low oxide remains in an 8090–SP diffusion bonded.

where the alloy grain boundaries intercept the bond line, they form 120° angle triple points. These triple points occur in spite of their high resistance to migration. Discrete particles, analysed by EDX as oxide compounds, were observed in zones close to these grain boundaries in the original position occupied by the bond interface.

4. Discussion

The present microstructural results confirm that there are two main factors differing in the solid state bonding of AA8090 compared with other commercial free-Li aluminium alloys:

1. the presence of Li favours partial disruption and elimination of the alumina film by forming less stable lithium-rich Al spinels, and
2. the great microstructural stability of the parent alloy caused by the presence of Al_3Zr particles (β' phase) hinders bonding interface migration and its recrystallization.

The diffusion bonding process studied in this paper takes the advantages derived from the first of these phenomenon, and limits the second. Using an

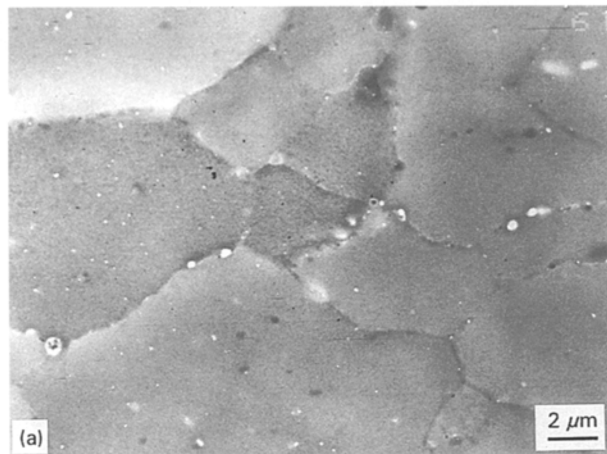

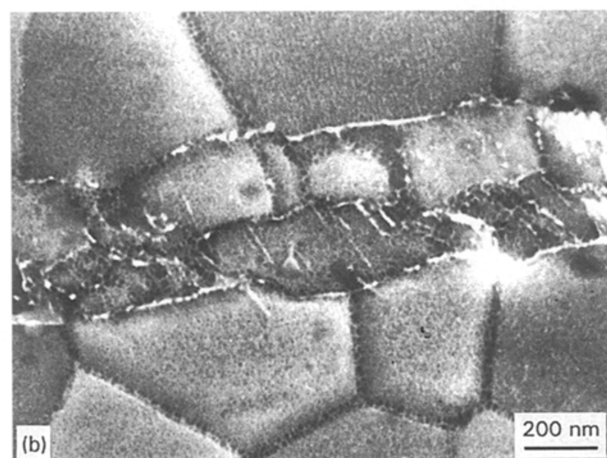

Figure 24 (a) Zone of interlayer elimination with recrystallization across bond interface, and (b) interlayer microstructure in a low deformed 8090–SP joint.

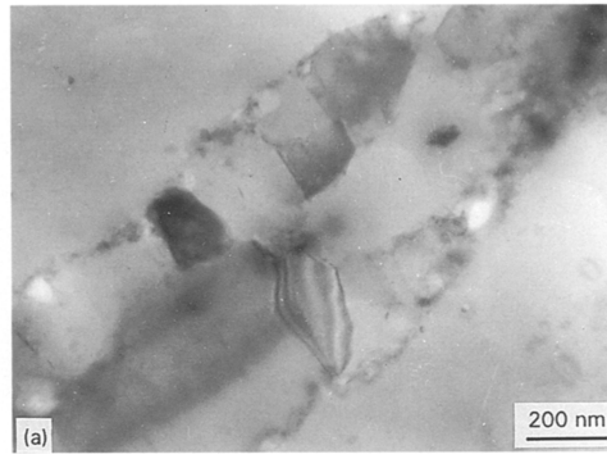

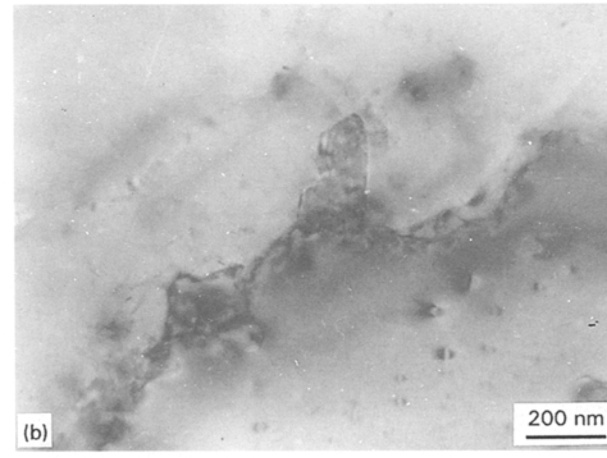

Figure 25 TEM micrographs of 8090–SP diffusion bonds: (a) interlayer recrystallization, and (b) bond interface with elimination of interlayer and formation of new subgranular structures.

interlayer of Al–4% Cu, which is chemically compatible with the parent alloy, a Li composition gradient is created in the bonding zone. It acts as the driving force for the diffusion processes and favours subsequent reaction with the alumina film. The elimination of this diffusion barrier is accelerated by the operation of chemical cleaning with commercial aluminium deoxidant, which is applied before bonding. Under these conditions, the formation of a solid state joint with a low proportion of interfacial oxide is possible, appearing only as discrete oxide particles in the bond interface.

However, the diffusion bonding trials have shown that there are two additional parameters which are involved in the formation of an oxide-free interfacial joint: (1) the increase of bonding pressure, and (2) the decrease of oxygen partial pressure in the bonding atmosphere. For the bonding conditions applied (530 °C and 10–30 min), it is necessary to apply bonding pressures of about 4 MPa for the superplastic alloy, and 5.5 MPa for T6 alloy. The oxygen partial pressure must be limited to values lower than 2×10^{-2} Pa to avoid serious problems of interface oxidation.

SEM and TEM studies of specimens bonded at optimum conditions show that the Al–Cu interlayer, applied by vapour deposition, can recrystallize forming a subgrain structure similar to the parent alloy. This recrystallization phenomenon can spread out along the bond interface and affect the parent alloy grains next to it, in spite of the migration resistance caused by the pinning effect of Al_3Zr particles. It has been observed that the recrystallization phenomenon occurs more easily in the superplastic alloy. In this case, local elimination of the bond interface may be associated with the processes of dynamic recrystallization produced by intensive plastic deformation generated in these zones during bonding.

The higher degree of homogenization observed in the joined superplastic sheets compared with the T6 sheets, is a consequence of the smaller grain size of that material accelerating grain boundary diffusion. Besides, its higher deformability favours local disruption of the alumina film by mechanical mechanisms, together with the local dynamic recrystallization previously discussed. However, it makes it difficult to obtain high quality joints for these alloys by the diffusion bonding method studied, if the bonding deformation is less than 25%.

In spite of those local phenomena, the bonding interface is characterized by high planarity and has a structure similar to the large-angle grain boundaries present in the sheet. Although discrete oxide particles appear at the planar bond interface, in this state they

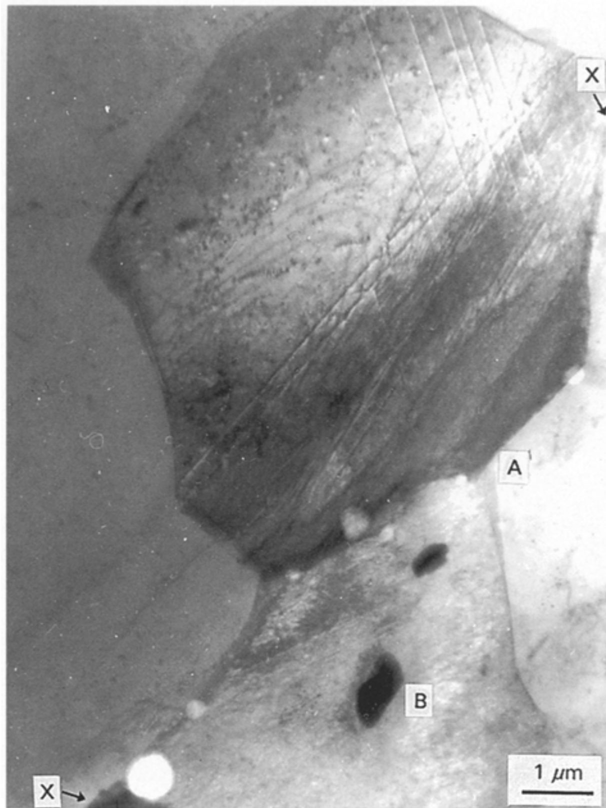

Figure 26 TEM micrograph of an interface at X–X showing several triple joints (A), and some oxide remains (B).

have no apparent effect on its low mobility and are unable to cause the pinning effect of Al_3Zr particles.

Another advantage of the studied bonding method is that microstructural stability of the parent alloys is guaranteed because of the short bonding times used. For the superplastic alloy, the grain size is kept in a range necessary to guarantee the superplastic properties. In the same way, the bonding condition used limits the surface oxidation problems, although surface lithium depletion occurred by sublimation.

5. Conclusions

1. A diffusion bonding method has been developed for the 8090 aluminium–lithium alloy, using an Al–4% Cu interlayer obtained by vacuum vapour deposition, at a bonding temperature of 530 °C; pressure, 4–5.5 MPa; times in the range 10–30 min; and a bonding atmosphere with partial oxygen pressure lower than 2×10^{-3} Pa.

2. For previous bonding conditions, elimination of the continuous interfacial oxide layer is possible, and only discrete oxide particles (probably Li-rich spinels) are detected in the bond interface. This oxide elimination is accelerated if the bonding surface are chemically cleaned with a commercial deoxidant.

3. In spite of the stability and high resistance to migration of the bonding interface, it is possible to obtain zones of local recrystallization, especially in superplastic joined sheets. It is probably due to mechanisms of local dynamic recrystallization associated with highly deformed zones.

4. The thermal bonding cycles applied to the alloys does not cause serious surface oxidation problems, although surface lithium depletion occurs by sublimation. Besides, the grain size of the superplastic alloy is kept in the range necessary for superplastic behaviour.

Acknowledgements

The authors thank the Comision Interministerial de Ciencia y Tecnología (CICYT) for its financial support for the realization of the present research (Project No. MAT 91/0033).

References

1. L. ASCANI, in “Proceedings of the ASM Materials Conference on Innovations in Materials and their Applications”, Chicago, 1987 (American Society for Metals, Metals Park, OH, 1977) p. 19.
2. J. R. WILLIAMSON, in “Proceedings of the Conference on Welding Technology for the Aerospace Industry”, Las Vegas, Oct., 1980. (American Welding Society, Miami, 1981) p. 53.
3. D. V. DUNFORD and P. G. PARTRIDGE, in “Proceedings of the Conference on Superplasticity in Aerospace–Aluminium”, edited by Pearce and L. Kelly, Crandfield, 1985. (CIT, Crandfield, 1985) p. 252.
4. E. J. LAVERNIA and N. J. GRANT, *J. Mater. Sci.* **22** (1987) 1521.
5. J. PILLING, “Superplasticity and Superplastic Forming” (TMS, American Institute of Mining, Metallurgy and Petroleum Engineers, Warrendale, PA 1988) p. 475.
6. M. R. EDWARDS, E. KLINKIN and V. E. STONEHAM, in “Proceedings of the Conference on Aluminium–Lithium Alloys V” (Williamsbourg, March 1989) E. A. Starke Jr. and T. H. Sanders (Eds) *Materials and Components Engineering*, Warley (1989), p. 431.
7. P. G. PARTRIDGE, *Int. Metall. Rev.* **35** (1990) 37.
8. A. UREÑA and S. B. DUNKENTON, “Diffusion Bonding of an Aluminium–Lithium Alloy (AA8090)” TWI Report No. 403/1989 (The Welding Institute, Abington, 1989).
9. A. UREÑA, J. M. GOMEZ DE SALAZAR and J. QUIÑONES, in “Proceedings of the Conference on Eurojoining” (ECCW-Institut de Soudure, Strasbourg, 1991) p. 401.
10. A. ARUN JUNAI, M. SCHANSSEMA and J. H. MAAS, in “Joining/Welding 2000, Proceedings of Conference IIW,” The Hauge, July 1991 (Pergamon, Oxford, 1991) p. 312.
11. R. A. RICKS, P. J. WINKLER, M. JROKLOSSA and R. GRIMES, in “Proceedings of the Conference on Aluminium–Lithium Alloys V”, edited by E. A. Starke Jnr. and T. H. Sanders (Materials and Components Engineering Warley, 1989) p. 447.
12. C. J. GILMORE, D. V. DUNFORD and P. G. PARTRIDGE, *J. Mater. Sci.* **26** (1991) 3119.
13. K. T. VENKATESWARA RAO and R. O. RITCHRE, *Mater. Sci. Technol.* **5** (1989) 882.
14. R. J. LEDERICH and S. H. L. SASTRY, in “Proceedings of the Conference on Aluminium–Lithium II”, edited by E. A. Starke Jnr. and T. H. Sanders, Monterray, 1983. (TMS-AIME, Warrendale, 1984).
15. J. WHITE, W. S. MILLER, J. G. PALMER, R. DAVIS and T. S. SAINI, in “Proceedings on the Conference on Aluminium-Lithium Alloys III”, Oxford, July, 1985, edited by C. Baker, P. Gregson, S. J. Harris and C. J. Peel (Institute of Metals, London, 1986) p. 530.
16. S. FOX, H. M. FLOWER, D. S. McDARMAID, in “Proceedings of the Conference on Aluminium–Lithium Alloys III”, *ibid.*, p. 263.
17. M. RADULLA, S. UDYAVAR and E. S. DWARAKADASA, *J. Mater. Sci. Lett.* **11** (1992) 490.
18. J. PILLING and N. RIDLEY, in “Superplasticity in cristalline solids” (The Institute of Metals, London, 1989) p. 3.

Received 7 January 1994
and accepted 11 May 1995